Nanoscale resolution fluorescence microscopy using electromagnetically induced transparency

D. D. Yavuz and N. A. Proite

Department of Physics, 1150 University Avenue, University of Wisconsin at Madison, Madison, Wisconsin 53706, USA

We suggest a type of scanning fluorescence microscope that is capable of resolving nanometer-size objects in the far field. The key idea is to use the spatial sensitivity of the dark state of electromagnetically induced transparency and localize an atomic excitation to a spot much smaller than the wavelength of light.

It is well known that, by using the nonlinear interaction between atoms and laser beams, one can localize atoms to a spot much smaller than the wavelength of light. In their pioneering work, Thomas and colleagues have suggested and experimentally demonstrated subwavelength position localization of atoms using spatially varying energy shifts [1–3]. If a very small object is embedded into an atomic medium, subwavelength atom localization can be used to obtain a shadow image of the object [2]. Recently, there has been a growing interest in various techniques of manipulation of atoms at the subwavelength scale. Zubairy and colleagues have discussed atom localization using resonance fluorescence and phase and amplitude control of the absorption spectrum [4–6]. Knight and colleagues discussed localization via quantum interference at the probability amplitude of the excited state [7]. There is also substantial literature on subwavelength localization of atoms utilizing excitation in a standing wave [8,9]. Although these are very exciting developments, a practical optical microscope utilizing nanoscale localization of atoms has not yet been demonstrated. If constructed, such a microscope may provide a unique way to image small objects, including large biological molecules at the nanometer scale. Although significant advances have been made in recent years, such as the invention of stimulated emission depletion microscopy [10], it is still a big challenge to map and understand the structure of single molecules.

In this Rapid Communication, we suggest a type of microscope that is based on tight localization of atoms. The key idea of our scheme is to localize atomic excitation to a spot much smaller than the diffraction limit, using the dark state of electromagnetically induced transparency. Our scheme is the extension of the suggestion of Agarwal and colleagues to tightly focused beams and utilizes adiabatic evolution instead of optical pumping [9]. As will be detailed below, a key advantage of our scheme is its insensitivity to fluctuations in experimental parameters. This is due to the robust nature of the adiabatic preparation of the dark state. Noting Fig. 1, we consider a nanometer-scale object embedded in an ultracold atomic medium with four atomic states. As an example, the atomic medium can be submillikelvin temperature alkali-metal atoms trapped in a magneto-optical trap (MOT) or in a far-off-resonant dipole trap. The idea of placing nanoscale objects inside an ultracold atomic cloud was motivated by recent experiments of Hakuta and colleagues where optical properties of a nanofiber inside a MOT were studied [11]. Two laser beams couple the two hyperfine states of the atom (states $|1\rangle$ and $|2\rangle$) to an excited electronic state (state $|3\rangle$)

and form a traditional Λ scheme. With an atom starting in the ground state $|1\rangle$, using a counterintuitive pulse timing sequence, the atomic system can be prepared in the dark state. When this is the case, the probability amplitudes of states $|1\rangle$ and $|2\rangle$ depend very sensitively on the ratio of the Rabi frequencies of the two laser beams, Ω_p and Ω_c. The nonlinearity of this dependence can be used to spatially localize the population of state $|2\rangle$ to a very tight spot. The fluorescence laser between states $|2\rangle$ and $|4\rangle$ then causes fluorescence from the localized excitation. As a result, by scanning the focusing lens, it becomes possible to obtain a fluorescence shadow image of the embedded object at the nanometer scale.

We proceed with a detailed description of our scheme. Noting Fig. 1, with the fluorescence laser turned off, the dark state of the atom is [12,13]

$$|\psi_{dark}\rangle = \frac{\Omega_c^*}{\sqrt{|\Omega_p|^2 + |\Omega_c|^2}}|1\rangle - \frac{\Omega_p^*}{\sqrt{|\Omega_p|^2 + |\Omega_c|^2}}|2\rangle. \quad (1)$$

From Eq. (1), the population of state $|2\rangle$ is $|\langle 2|\psi_{dark}\rangle|^2 = |\Omega_p|^2/(|\Omega_p|^2+|\Omega_c|^2)$ and gets larger as the ratio $|\Omega_c/\Omega_p|$ is decreased. This suggests that, in a region where the coupling laser goes through an intensity minimum and the probe laser goes through an intensity maximum, the population in state $|2\rangle$ can be localized very tightly. If we assume Gaussian focusing and take the spatial profiles of the two Rabi frequencies at the focus as $\Omega_p(x,y)=\Omega_{p,peak}\exp[-(x^2+y^2)/W_0^2]$, $\Omega_c(x,y)=\Omega_{c,peak}-\Omega_{c,peak}\exp[-(x^2+y^2)/W_0^2]$, where W_0 is the Gaussian spot size, it can be shown that in the limit $\Omega_{p,peak}\ll\Omega_{c,peak}$, the population of state $|2\rangle$, $|\langle 2|\psi_{dark}\rangle|^2$, will be localized to an approximate spot size of

$$W_{excitation} \approx W_0\sqrt{\frac{\Omega_{p,peak}}{\Omega_{c,peak}}}. \quad (2)$$

Here, we take the atoms to be cold enough such that their motion can be neglected during excitation with the probe and coupling lasers. From Eq. (2), it follows that the resolution of such a microscope is $(\lambda/2)\sqrt{\Omega_{p,peak}/\Omega_{c,peak}}$ and for $\Omega_{p,peak}\ll\Omega_{c,peak}$ the resolution is significantly smaller than the wavelength of light. Use of more complicated focusing schemes where the coupling field goes through a phase change around its minimum provides better scaling of the resolution, $(\lambda/2)\Omega_{p,peak}/\Omega_{c,peak}$, at the expense of significant complications at the excitation structure.
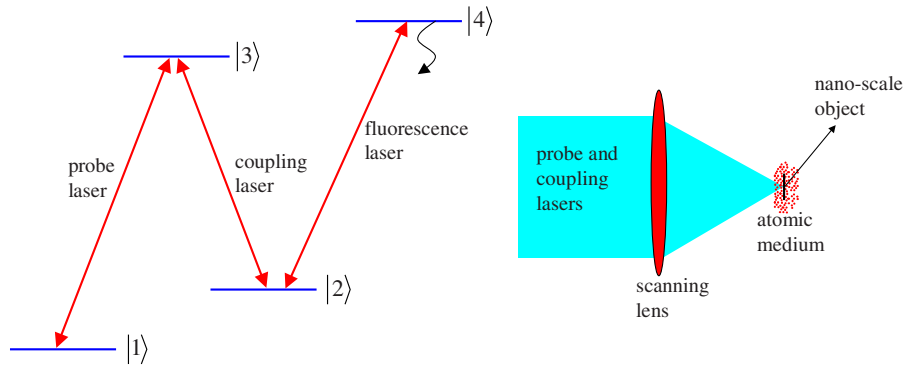
FIG. 1. (Color online) Energy level diagram and simplified schematic of the suggested technique. The probe and the coupling laser beams form a traditional Λ scheme and drive the atoms into the dark state. The sensitive spatial dependence of the dark state on the intensities of the two laser beams can be used to localize the population of state $|2\rangle$ to a spot much smaller than the diffraction limit. The fluorescence laser that scatters photons only when the atom is in state $|2\rangle$ may then be used to detect the tightly localized population. By scanning the focusing lens, a fluorescence shadow image of the embedded object at the nanometer scale is obtained.

We proceed with a numerical example in a real atomic system. We take our atomic medium to be ^{87}Rb and choose $|1\rangle \equiv |F=2, m_F=-2\rangle$ and $|2\rangle \equiv |F=1, m_F=0\rangle$ of the ground electronic state $5S_{1/2}$. We take the excited state to be $|3\rangle \equiv |F'=2, m_F=-1\rangle$ of the electronic state $5P_{1/2}$ (D_1 line with a transition wavelength of 795 nm). The decay rate of the excited state is $\Gamma = 2\pi \times 5.7$ MHz. We take the probe and coupling laser beams to be of opposite circular polarization (σ^+ for the probe and σ^- for the coupling). For this choice of state selection and polarization selection for the laser beams, the effect of the intense coupling laser on the ground state $|1\rangle$ (such as Stark shift and optical pumping) is negligible due to angular momentum selection rules. Since the two laser beams are focused tightly into the cloud, we need to consider vectorial properties of light to get an accurate distribution of the Rabi frequencies near the focus, $\Omega_p(x,y,z)$ and $\Omega_c(x,y,z)$. For this purpose, we use the formalism of Richards and Wolf [14]. We assume a semiaperture angle of $\alpha=60°$ for focusing and calculate the three-dimensional distribution of the electric field numerically. To obtain an intensity minimum in the profile of the coupling laser beam, we use the approach of Saffman and colleagues [15]. For this purpose we use two copropagating coupling laser beams, one tightly focused (with $\alpha=60°$) and one plane wave, and adjust their phases such that there is destructive interference at the focus. We note that one may use other methods for generating beams with an intensity minimum at the center [16]. A one-dimensional cross section along one of the transverse coordinates is shown in Fig. 2(b). We take the peak values for the Rabi frequencies of the two laser beams as $\Omega_{p,peak}=5\Gamma$ and $\Omega_{c,peak}=1000\Gamma$. When the coupling laser intensity vanishes, the dark-state solution of Eq. (1) is no longer valid. To avoid this, we adjust the focusing parameters such that the coupling laser Rabi frequency does not vanish at $x=y=0$ but instead drops to a low value of 5Γ. The system is, therefore, at the maximally coherent state at $x=y=0$.

With the spatial profiles for the Rabi frequencies known, we can calculate the fractional populations of the dark state as per Eq. (1). In Fig. 2(a), we plot the population fraction, $|\langle 2|\psi_{dark}\rangle|^2$, as a function of one of the transverse coordinates. For comparison, Fig. 2(b) shows the spatial profiles of

the Rabi frequencies of the two laser beams. Figure 2(c) is a zoom on the spatial profile of part (a). The population transfer to state $|2\rangle$ has a FWHM of 51.1 nm, which is about 15 times smaller than the wavelength of the laser beams, in rough agreement with the qualitative estimate of Eq. (2).

In Fig. 2, we assumed the ideal case and considered an atomic system in an exact dark state as given by Eq. (1). We next discuss temporal evolution of the atomic system. For this purpose, we numerically solve the Schrödinger equation for the probability amplitudes of the three states [17]. To prepare the atomic system in the dark state, we follow the
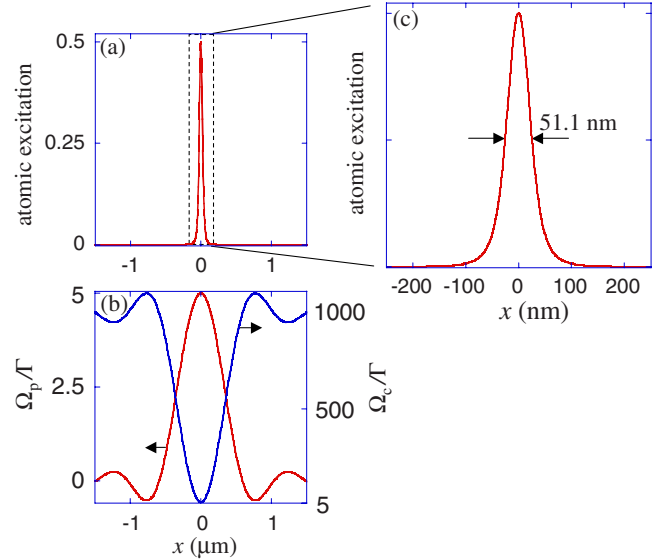

FIG. 2. (Color online) Localization of atomic excitation to a spot much smaller than the diffraction limit. (a) shows the atomic excitation $|\langle 2|\psi_{dark}\rangle|^2$, assuming that the atomic system is in the dark state given by Eq. (1). (b) shows the spatial distribution of the Rabi frequencies for the probe laser Ω_p and the coupling laser Ω_c, which results in the localization of (a). These distributions are calculated numerically by taking into account vectorial properties of light near a tight focus. (c) is a zoom on (a) detailing the spatial structure of the excitation. The excitation has a full width at half maximum (FWHM) of 51.1 nm, which is about 15 times smaller than the wavelength of light.
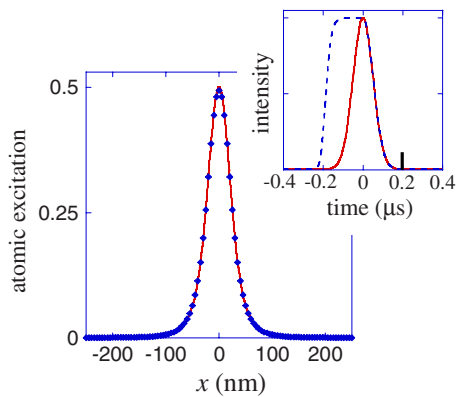
FIG. 3. (Color online) Numerical calculation that demonstrates localization with pulsed excitation. The inset shows the assumed temporal profiles for the intensities of the probe (solid) and coupling (dashed) laser beams. Starting from the ground state $|1\rangle$, we numerically integrate the Schrödinger equation at each spatial point along the profiles of the probe and coupling laser beams of Fig. 2(b). The data points are the fractional population $|\langle 2|\psi\rangle|^2$ at $t=0.2$ μs (shown with a tick mark in the inset) at each spatial point. The solid line is a replot of Fig. 2(c). There is good agreement between the results of the exact numerical simulation and the idealized calculation of Fig. 2.

well-known approach and use a counterintuitive pulse sequence [12,13]. As shown in the inset of Fig. 3, the coupling laser beam (dashed line) is turned on before the probe laser beam (solid line). For this type of preparation, the dark state is smoothly connected to the ground state and the atomic system is adiabatically prepared into the dark state. Once the laser beams are turned on, they can be turned off simultaneously, preserving the ratio of the Rabi frequencies. As a result, even after the laser pulses are gone, the atomic system is left in the state as determined by the probe and coupling laser Rabi frequencies at the temporal peak of the pulses.

Figure 3 shows an exact numerical simulation that confirms the predictions of the results of Fig. 2. Here, we solve the Schrödinger equation at each point in the spatial profiles of the probe and coupling laser beams of Fig. 2(b). The inset shows the assumed (normalized) temporal profiles for the intensities of the probe (solid) and coupling (dashed) laser beams. The probe laser is assumed to be a Gaussian pulse with a Gaussian width of $\tau=0.1$ μs. The coupling laser turns on before but turns off simultaneously with the probe laser. In the main plot, the data points are the fractional population $|\langle 2|\psi\rangle|^2$ at $t=0.2$ μs (shown with a tick mark in the inset) at each spatial point. The solid line is a replot of Fig. 2(c). We observe very good agreement between the exact numerical simulation and the idealized calculation of Fig. 2. Once the probe and the coupling lasers are switched off ($t>0.2$ μs), the fluorescence laser is switched on. The fluorescence laser does not need to be spatially selective and it can have a large spot size. The motion of the atoms during the fluorescence process is not of importance. By scanning the focusing lens and by repeating the pulsed excitation-fluorescence detection cycle at each scanning point, the fluorescence image of the embedded object is obtained.
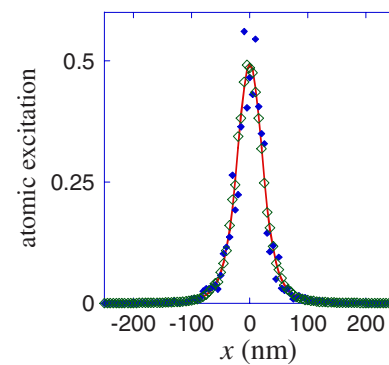

FIG. 4. (Color online) Numerical simulations that demonstrate the robust nature of our scheme. For the open squares, the intensity of the coupling laser beam fluctuates by ±10% at each scanning point. For the solid squares, a timing jitter of ±0.01 μs is assumed between the probe and coupling laser pulses. All the other parameters are identical to those of Fig. 3. The solid line is a replot of the numerical simulation of Fig. 3.

A significant advantage of our approach is its insensitivity to fluctuations in many experimental parameters. This is due to the robust nature of adiabatic preparation and is also the key reason for the success of the technique of stimulated Raman adiabatic passage (STIRAP) [18]. Figure 4 demonstrates this result. Here, the solid line is a replot of the numerical simulation of Fig. 3. For the open squares, with all other parameters identical to those of Fig. 3, the intensity of the coupling laser beam fluctuates by ±10% at each scanning point. For the solid squares, a timing jitter of ±0.01 μs is assumed between the probe and coupling laser pulses. For both cases, the numerical results are very close to the profile when there is no fluctuation (solid line) proving the insensitivity of the resolution.

A significant limitation of atom-localization-based microscopes is the scanning speed. For the numerical example considered, the atomic excitation at each scanning point will be localized to a volume of 2×10^{-16} cm^3. Current laser cooling and trapping techniques allow ultracold atomic densities exceeding $N=10^{14}$ atoms/cm^3 [19]. For such densities, a guaranteed excitation of at least one atom requires about $1/(NV)\approx 50$ pulsed excitation-fluorescence detection cycles at each scanning point. Since detection of a single atom with a good signal-to-noise ratio requires about 10 ms integration time [20–22], this means that each scanning point with the resolution of Fig. 2 would require about 0.5 s of integration time. This limitation can be overcome by using faster state-selective detection techniques. One approach could be to use state-selective ionization followed by ion detection. Such approaches can reduce the required integration time for each scanning point to below 1 ms.

Throughout this Rapid Communication, we have assumed the atoms to be cold enough such that their motion can be neglected during the adiabatic excitation with the probe and the coupling laser beams. For an excitation time of $\tau=0.1$ μs this assumption is satisfied for alkali-metal atoms that are cooled to about 50 μK which is readily achievable with sub-Doppler cooling in optical molasses. For the numerical results of Fig. 3, we calculate the heating of the

atoms during the pulsed excitation with the probe and coupling lasers to be negligible. The required laser power for the experimental observation of the results of Figs. 2 and 3 are low (<1 mW), and are readily achievable with available diode lasers. Throughout this Rapid Communication, we have also neglected the interaction of the object with the atomic cloud. The dominant force between the neutral atoms and the embedded object at short separations ($r < 1$ μm) is the van der Waals force. The strength of the van der Waals interaction between alkali-metal atoms and surfaces is well studied [23–25]. If we assume that the surface is an infinite planar surface, we estimate the frequency shift of the ground and the excited states to be at the megahertz level for atom-surface separation of $r = 50$ nm. Since this shift is much smaller than the Rabi frequencies of the probe and the coupling laser beams, we do not expect significant corrections to the results presented in this paper due to atom-surface interactions. However, for $r = 10$ nm, the transition shifts and the heating of the atoms become significant. These effects need to be carefully taken into account, for resolutions below 10 nm. In principle, these effects can be overcome by using larger Rabi frequencies for the probe and the coupling laser beams and using shorter excitation pulses [26].

We envision that the first experimental demonstration of our approach may use a nanoscale object such as a carbon nanowire inside the Rb cloud. These experiments will be very much in the spirit of recent experiments by Hakuta and colleagues where a nanofiber was placed inside a magneto-optical trap of ultracold atoms and the optical properties of atoms near the nanofiber were studied [11]. In these experiments, no significant heating of the ultracold atomic cloud was observed. Another exciting direction would be if such a microscope can be used to image large biological molecules at the nanometer scale. We envision grabbing a biological molecule of interest with an optical tweezer and overlapping it with the atomic cloud. Our approach may also provide a unique way to atomic lithography with resolution well into the nanometer scale [27].

Note added. Recently, we became aware of a related proposal by Lukin and colleagues that utilizes spatial dependence of the dark state to achieve coherent quantum control with subwavelength resolution [28].

[1] J. E. Thomas, Opt. Lett. **14**, 1186 (1989).

[2] K. D. Stokes *et al.*, Phys. Rev. Lett. **67**, 1997 (1991).

[3] J. R. Gardner, M. L. Marable, G. R. Welch, and J. E. Thomas, Phys. Rev. Lett. **70**, 3404 (1993).

[4] F. Le Kien, G. Rempe, W. P. Schleich, and M. S. Zubairy, Phys. Rev. A **56**, 2972 (1997).

[5] S. Qamar, S. Y. Zhu, and M. S. Zubairy, Phys. Rev. A **61**, 063806 (2000).

[6] M. Sahrai, H. Tajalli, K. T. Kapale, and M. S. Zubairy, Phys. Rev. A **72**, 013820 (2005).

[7] E. Paspalakis and P. L. Knight, Phys. Rev. A **63**, 065802 (2001).

[8] J. Xu and X. Hu, J. Phys. B **40**, 1451 (2007).

[9] G. S. Agarwal and K. T. Kapale, J. Phys. B **39**, 3437 (2006).

[10] S. W. Hell and J. Wichmann, Opt. Lett. **19**, 780 (1994).

[11] K. P. Nayak, P. N. Melentiev, M. Morinaga, Fam Le Kien, V. I. Balykin, and K. Hakuta, e-print arXiv:quant-ph/0610136.

[12] M. O. Scully and M. S. Zubairy, *Quantum Optics* (Cambridge University Press, Cambridge, U.K., 1997).

[13] S. E. Harris, Phys. Today **50**(7), 36 (1997).

[14] B. Richards and E. Wolf, Proc. R. Soc. London, Ser. A **253**, 358 (1959).

[15] L. Isenhower and M. Saffman, in Proceedings of DAMOP 2007, Calgary, Canada (unpublished).

[16] J. Arlt and M. J. Padgett, Opt. Lett. **25**, 191 (2000).

[17] S. E. Harris and Z. F. Luo, Phys. Rev. A **52**, R928 (1995).

[18] K. Bergmann, H. Theuer, and B. W. Shore, Rev. Mod. Phys. **70**, 1003 (1998).

[19] R. Newell, J. Sebby, and T. G. Walker, Opt. Lett. **28**, 1266 (2003).

[20] N. Schlosser, G. Reymond, I. Protsenko, and P. Grangier, Nature (London) **411**, 1024 (2001).

[21] D. Schrader *et al.*, Phys. Rev. Lett. **93**, 150501 (2004).

[22] D. D. Yavuz *et al.*, Phys. Rev. Lett. **96**, 063001 (2006).

[23] V. Sandoghdar, C. I. Sukenik, E. A. Hinds, and S. Haroche, Phys. Rev. Lett. **68**, 3432 (1992).

[24] J. D. Perreault and A. D. Cronin, Phys. Rev. Lett. **95**, 133201 (2005).

[25] A. O. Caride, G. L. Klimchitskaya, V. M. Mostepanenko, and S. I. Zanette, Phys. Rev. A **71**, 042901 (2005).

[26] B. E. Unks, N. A. Proite, and D. D. Yavuz, Rev. Sci. Instrum. **78**, 083108 (2007).

[27] K. S. Johnson *et al.*, Science **280**, 1583 (1998).

[28] A. V. Gorshkov, L. Jiang, M. Greiner, P. Zoller, and M. D. Lukin, e-print arXiv:quant-ph/0706.3879.